Missouri University of Science and Technology
Scholars' Mine

Materials Science and Engineering Faculty Research & Creative Works

Materials Science and Engineering

01 Mar 1990

Electrochemical Evaluation Of Copper Deposition With Gas Sparging

D. A. Uceda

Thomas J. O'Keefe
Missouri University of Science and Technology

Follow this and additional works at: https://scholarsmine.mst.edu/matsci_eng_facwork

 Part of the Metallurgy Commons

Recommended Citation

D. A. Uceda and T. J. O'Keefe, "Electrochemical Evaluation Of Copper Deposition With Gas Sparging," *Journal of Applied Electrochemistry*, vol. 20, no. 2, pp. 327 - 334, Springer, Mar 1990.
The definitive version is available at https://doi.org/10.1007/BF01033612

This Article - Journal is brought to you for free and open access by Scholars' Mine. It has been accepted for inclusion in Materials Science and Engineering Faculty Research & Creative Works by an authorized administrator of Scholars' Mine. This work is protected by U. S. Copyright Law. Unauthorized use including reproduction for redistribution requires the permission of the copyright holder. For more information, please contact scholarsmine@mst.edu.

JOURNAL OF APPLIED ELECTROCHEMISTRY 20 (1990) 327–334

Electrochemical evaluation of copper deposition with gas sparging

D. A. UCEDA, T. J. O'KEEFE

Department of Metallurgical Engineering and Materials Research Center, University of Missouri-Rolla, Rolla, MO 65401, USA

Received 6 April 1989; revised 5 June 1989

The influence of gas sparging during copper electrolysis was studied using standard electrochemical techniques. The polarization behaviour of acid copper electrolytes was determined in the presence and absence of gas sparging on vertical electrodes. Tracer ion techniques were employed to determine the effect of gas sparging and forced circulation of the electrolyte on the mass transfer characteristics of the system. In addition to the potentiodynamic scans, 3-h copper deposits were produced for morphology and orientation studies. The effect of current density and temperature on deposition were also studied. The polarization experiments have shown that a mass transfer component becomes evident at about 40% of the limiting current density at which point the deposit becomes noticeably rougher.

1. Introduction

The rate of an electrochemical process is measured by the current density flowing in a cell. It is generally desirable economically to have as high a current density as possible [1] and various methods for increasing the current have been proposed. Agitation of the electrolyte has been found to increase the limiting current density when concentration polarization is a factor. Several forms of agitation have been used, including forced circulation across the cathode by pumping electrolyte (effective but expensive), ultrasonic agitation (which requires significant amounts of energy and produces a considerable noise level), and gas sparging which is the subject of the present study.

Recently, interest in the use of gas sparging in copper electrolysis has increased [2, 3]. Gas sparging has certain advantages over the conventional electrolytic process such as improving cathode quality and allowing a higher rate of production. The fundamental reasons for the improvement are most probably due to the increased mass transport and limiting current density that result.

Attempts to achieve better mass transport characteristics and improve cathode quality, in both electrowinning and refining, by means of gas sparging have been reported by several investigators [4].

Since mass transport plays such a vital role in copper electrolysis, a knowledge of the Cu^{2+} limiting current density is desirable, but it is not easily obtained, particularly in actual practice, because of the increasing surface roughness when plating close to the limiting current density. Surface changes and non-uniformity of flow over the cathode are partly responsible. To overcome this problem a technique [5–7] was developed using a tracer ion which was co-deposited with the copper. The tracer must have a more noble potential than the major reducible species (Cu^{2+}) and deposit at its limiting current density throughout the deposition cycle. The limiting current density of the tracer was obtained either by chemical analysis or by direct electrochemical measurement. Subsequently, the mass transfer coefficient of the tracer can be calculated by

$$K = I_L/(nFC_b) \quad (1)$$

K is the diffusion mass transfer coefficient of the tracer ($cm\,s^{-1}$), I_L is the limiting current density ($mA\,cm^{-2}$), n is the change of oxidation state, F is the Faraday constant (coulombs per equivalent) and C_b is the concentration of the tracer in the bulk electrolyte ($mol\,cm^{-3}$).

The mass transfer coefficient of the main component (Cu^{2+} in this case) can then be calculated using the relationship

$$K_{Cu^{2+}} = K_T(D_{Cu^{2+}}/D_T)^m \quad (2)$$

$D_{Cu^{2+}}$ and D_T are the diffusion coefficient of Cu^{2+} and the tracer, respectively ($cm^2\,s^{-1}$), m has the value of $\frac{3}{4}$ for natural convection in a laminar regime, and $\frac{2}{3}$ for other flow regimes.

Other mass transfer related properties of the main ion, such as the limiting current density and diffusion layer thickness, can also be estimated by Equation 1 and

$$\delta = D/K \quad (3)$$

The concentration of copper at the electrode/electrolyte interface can be estimated for conditions less than the limiting current density by the following expression

$$C_0 = C_b - I/nFK \quad (4)$$

In this study, the limiting current density of the tracer was potentiodynamically measured in Cu/H_2SO_4 electrolytes. The limiting current was determined from the cyclic voltammograms, and the mass transfer

0021-891X/90 $03.00 + .12 © 1990 Chapman and Hall Ltd.

properties of the electrolyte were evaluated. Using this technique, the natural convection is negligible since the concentration of the tracer is sufficiently low to prevent density changes of the electrolyte at the electrode surface. Thus the enhancement of mass transfer due to natural or forced convection during codeposition of the tracer and copper could be determined by comparing these two values.

When the tracer was codeposited with copper, the Cu^{2+} concentration at the cathode interface was reduced. Natural convection due to differences in electrolyte density would be expected and enhanced mass transport would result. Wilke *et al.* [8] correlated the Sherwood number to the Grashof and Schmidt numbers for a laminar natural convection by the equation

$$Sh = 0.673\ (Sc\,Gr)^{1/4} \quad (5)$$

Sh is the Sherwood number ($Sh = KL/D$), Gr is the Grashof number [$Gr = gL^3(\varrho_b - \varrho_0)/(\varrho_0 \nu^2)$], Sc is the Schmidt number ($Sc = \nu/D$), L is the electrode height (cm), ϱ_b is the density of the bulk electrolyte ($g\,cm^{-3}$), ϱ_0 is the density of the electrolyte at electrode/electrolyte interface ($g\,cm^{-3}$) and ν is the kinematic viscosity ($cm^2\,s^{-1}$).

The experimentally determined Sherwood number, Sh', can be calculated ($Sh' = L/\delta$) and compared with the predicted Sherwood number.

When the flow regime is increased a different correlation is expected. Based on the Chilton–Colburn analogy, it has been shown that for a fully developed turbulent flow of electrolyte [10] the following equation is valid

$$I_{Lim} = \text{const} \times Re^{0.8} \quad (6)$$

where, Re is the Reynolds number.

2. Experimental

For electrochemical measurements, the experimental arrangement consisted of vertical metal electrodes in a 400 ml beaker fitted with a plastic cover. The potentiodynamic measurements were made using a platinum wire as a counter electrode, which was made into a spiral and placed in a glass tube with a fritted end which dipped into the solution. With this construction the oxygen evolved did not affect the hydrodynamic state of the solution. A Hg/Hg_2SO_4 (saturated K_2SO_4) reference electrode with a potential of 0.664 V (SHE) at 25° C was used. For mass transport determinations, the working electrode was a platinum square of 1 cm^2 polished with 0.05 μm gamma alumina and then rinsed with distilled water. Electrolytes contained 36 $g\,l^{-1}$ Cu^{2+} and 143 $g\,l^{-1}$ H_2SO_4. The solution was prepared from certified grade cupric sulphate pentahydrate and reagent grade sulphuric acid. The solution temperature was maintained at 25° C (unless otherwise stated) using a thermostated water flow through the jacketed cell. The potential scanning range was from −0.1 to −0.3 V w.r.t. a Hg_2SO_4 reference electrode and the scan rate was 0.5 $mV\,s^{-1}$. In this potential range, only the Ag^+ tracer was deposited and the limiting current density of Ag^+ was directly determined from the limiting current plateau observed in the voltammogram. For gas sparging, both fritted glass and a capillary delivery tube were used.

The potentiodynamic polarization and cyclic voltammetry measurements were carried out using a Petrolite M-4100 Potentiodyne Analyser. Silver codeposition was used to evaluate the mass transport characteristics of the solution, assuming only natural convection during the copper deposition. The deposits were then dissolved in 5 N HNO_3 and analysed by atomic absorption (A.A.) spectroscopy. The limiting current densities of Ag^+ were calculated by Faraday's law from the analysed amount of silver in the deposit for deposition times of 20 min.

For the cyclic voltammmetry experiments, the cathode was fabricated from a high purity copper rod with a circular cross-sectional area of 0.722 cm^2. This working electrode was polished with 600 grit paper prior to all runs. The voltammograms were started at the Cu/Cu^{2+} rest potential and driven in a cathodic direction to a pre-set maximum potential followed by a return to the initial potential at a scan rate of 0.5 $mV\,s^{-1}$.

Morphological studies were made on galvanostatically produced deposits using electrolytically refined copper as the soluble anodes. The cathode was a commercial titanium sheet with a working area of 4 cm by 3 cm and prepared by polishing on 600 grit paper. Teflon strips were used to prevent back and edge growth. One anode and one cathode were used, and a slotted Plexiglas top cover maintained a cathode to anode distance of 3 cm. The deposition time varied with current density, which was in the range from 20 to 50 $mA\,cm^{-2}$, to give a constant number of coulombs. The morphology of the deposits was determined by scanning electron microscopy (SEM).

3. Results and discussion

3.1. *Mass transfer determinations*

3.1.1. Natural convection. The Cu^{2+} mass transfer coefficient was determined as a function of the current density applied in order to estimate its relative increase due to the effect of natural convection. Table 1 shows the results obtained when the current density was varied from 5 to 40 $mA\,cm^{-2}$ at 25° C. The Ag^+ mass transfer coefficient was calculated using Equation 1 as well as the Cu^{2+} mass transfer coefficient using Equation 2. The diffusion coefficients of Ag^+ and Cu^{2+} were determined using rotating disc techniques. When Ag^+ is codeposited with copper, at increasing current densities, the forces generated by the natural convection will enhanced the Ag^+ mass transfer coefficient.

Table 1 shows the depletion of copper concentration at the electrode surface as the current density is increased, calculated using Equation 4. Extrapolation to zero concentration corresponds to the maximum

Table 1. Estimation of mass transfer parameters of Cu^{2+} electrodeposition using the codeposition of a Ag^{+} tracer at 25° C and various current densities

CD ($mA\,cm^{-2}$)	$K_{Ag+} \times 10^4$ ($cm\,s^{-1}$)	$K_{Cu2+} \times 10^4$ ($cm\,s^{-1}$)	$C_{0,t}$ ($mol\,l^{-1}$)	δ_{Cu2+} (μm)	$[K/K^0]_{Ag+}$
5	5.4	2.7	0.47	176	2.1
10	6.7	3.4	0.41	143	2.5
15	7.4	3.7	0.36	129	2.8
20	8.2	4.1	0.31	117	3.1
25	9.0	4.5	0.28	107	3.4
30	9.1	4.6	0.22	106	3.4
35	10.1	5.1	0.21	95	3.8
40	10.2	5.1	0.16	94	3.9

rate of deposition at which an electrochemical process can be carried out for a given hydrodynamic condition (in this case under natural convection) and is assumed to correspond to the limiting current density (Fig. 1). The limiting current was estimated to be 67 mA cm^{-2} at 25° C. The limiting current of the tracer was obtained from polarization curves and corrected, when necessary, for the residual current. The mass transfer coefficient was calculated to be $K^0 = 2.6 \times 10^{-4}$ cm s^{-1}.

The K^0 values were increased by a factor of 2.1 to 3.9 in the codeposition current density range investigated (from 5 to 40 mA cm^{-2}) when compared with the value potentiodynamically obtained in the absence of copper deposition. This enhancement is due to the increase of the concentration gradient across the diffusion layer at higher current densities. As a result, the natural convection caused by the difference in electrolyte density is also increased. In copper refining, in spite of the flow velocities involved, natural convection is an important, and relatively efficient, way of stirring. The corresponding thickness of the diffusion layer, in the range of current densities investigated, was decreased by one-half, from 176 to 94 μm at 25° C owing to natural convection. With the present experimental arrangement, the estimated diffusion layer thicknesses were lower than the values reported for a full size cathode. The value of the diffusion layer thickness obtained for a current density of 20 mA cm^{-2} was 147 μm while a value of 300 μm has been reported for the lower half of a 1 m high electrode [5].

In this study, an electrode of 1 cm^2 was used for mass transfer determinations, but for 3 h deposits an electrode of 12 cm^2 was used. For this purpose, a variation of the codeposition method was studied; the Ag^+ tracer was stirred into 250 cc of electrolyte to give 40 p.p.m. and a titanium sheet with an exposed area of 12 cm^2 was the cathode. The anode was a platinum wire inserted into a fritted glass tube. The copper deposition was conducted at 35 mA cm^{-2} and the electrolyte was sampled every 30 min over 3 h and analysed by atomic absorption for the remaining silver. The silver deposition occurs at the limiting current density according to Equation 1 and the rate of change is $d[Ag^+]/dt = K([Ag^+]A/V$. The integrated form is the first order rate expression

$$\ln \{[Ag^+]/[Ag^+]_0\} = KAt/V \qquad (7)$$

A is the cathodic area (cm^2), V the electrolyte volume (cm^3), t is the deposition time (s), $[Ag^+]_0$ is the initial concentration of silver and $[Ag^+]$ is the silver concentration at a given time. From the plot of the data in the form expressed by Equation 7, the slope, K, was obtained and δ was calculated using Equation 3. The values of δ range from 140 to 200 μm, which is somewhat higher than the value of 119 to 142 μm estimated for a 1 cm^2 platinum electrode using 35 mA cm^{-2}.

The experimental Sherwood number agrees with the predicted value following Wilke's approach for natural convection as shown in Table 2. The plating current density of the Cu–Ag codeposition is I. $I_{L,Ag+}$, K_{Ag+} and K_{Cu2+} are calculated by Equations 1 and 2 and C_0 of copper was calculated by Equation 3. ϱ_b and ϱ_0 were calculated using equations given in [9]. Sh' is the predicted value calculated using Equation 5, assuming natural laminar convection.

3.1.2. Forced circulation. One way of enhancing the mass transfer is by forced convection of the electrolyte in the vicinity of the cathode. In this study, the electrolyte was jetted upwards at different velocities across a platinum cathode of approximately 1 cm^2 in area. The tests were made at 25° C and a Ag^+ tracer was used to measure the changes potentiodynamically. A platinum mesh counter electrode was used. The poten-

Table 2. Calculation of Gr, Sc, Sh and Sh' numbers for electrodeposition of copper under natural convection at 25° C

I (mA cm^{-2})	5	10	15	20	25	30	35	40
$I_{L,Ag+} \times 10^5$ (A cm^{-2})	1.0	1.2	1.3	1.4	1.6	1.6	1.7	1.8
$\varrho_b - \varrho_0$ (g cm^{-3})	0.007	0.016	0.023	0.029	0.034	0.042	0.044	0.050
$Gr \times 10^{-3}$	34	76	115	146	171	211	221	254
Sc	2723	2723	2723	2723	2723	2723	2723	2723
Sh	57	70	78	86	94	95	106	107
Sh'	66	81	89	95	99	104	105	109

Table 3. Influence of electrolyte circulation on the mass transfer parameters using the potentiodynamic measurement of a Ag^+ tracer

Flow ($cc\,min^{-1}$)	$K_{Ag+} \times 10^4$ ($cm\,s^{-1}$)	$K_{Cu2+} \times 10^4$ ($cm\,s^{-1}$)	$I_{L,Cu2+}$ $mA\,cm^{-2}$	$[K/K^0]_{Ag}$	δ_{Cu2+} (μm)	I_L/I_L^0
48	13.5	8.2	89	5.1	59	1.3
70	22.2	13.4	145	8.4	36	2.2
96	31.1	18.9	204	11.8	26	3.0
140	41.9	25.4	275	15.9	19	4.1
194	59.4	36.1	390	22.6	13	5.8
232	72.9	44.3	479	27.7	11	7.1

tial was scanned at $1\,mV\,s^{-1}$ from -0.1 to $-0.3\,V$ against the Hg/Hg_2SO_4 reference electrode. The Ag^+ limiting current was arbitrarily taken from the limiting current plateau in the voltammogram at a potential of $-0.225\,V$. From the potentiodynamically measured limiting current densities of Ag^+, the mass transfer coefficients of Ag^+ and Cu^{2+} were calculated as well as the limiting current of Cu^{2+} and the corresponding diffusion layer thickness for different electrolyte flow rates (see Table 3 and Fig. 3).

The potentiodynamically measured I_{L,Ag^+}, the calculated mass transfer coefficient, as well as the data of zero codeposition current density (pure silver diffusion K^0) are included in Table 3. The limiting mass transport of Ag^+ was increased by a factor of 5.1 to 27.7 when the electrolyte flow rate was varied from 48 to $232\,cc\,min^{-1}$. I_L/I_L^0 is enhanced from 1.3 to 7.1 in the range of flow rates investigated. The flow rates have to be relatively high in order to obtain a diffusion layer thickness below $20\,\mu m$. Taking the 0.01 m height of the cathode as the characteristic length and knowing the kinematic viscosity of the electrolyte at 25° C ($\nu = 0.0131\,cm^2\,s^{-1}$), the Reynolds number was calculated for every speed of electrolyte flow. A plot of the diffusion limiting current density of Cu^{2+} (in $mA\,cm^{-2}$) against the Reynolds number shows that for *Re* numbers larger than 2000 the power of 0.8 in the Reynolds number term gives a better fit, which can be compared with powers of 0.8 of the Chilton–Colburn analogy [10] and 0.9 of the Vielstich law [11] developed for mass transfer in turbulent flow (see Fig. 2).

3.1.3. Gas sparging. For the mass transport determinations using gas sparging, the experimental arrangement was similar to that used for forced circulation of the electrolyte. Gas sparging was provided through a fritted glass sparger or a single bubble tube sparger located directly below the platinum electrode. The experimental mass transfer parameters obtained at 25° C are shown in Table 4 using Ag^+ as a tracer. It is observed that even a lower gas flow rate such as $22\,cc\,min^{-1}$ produces a large mass transport enhancement of silver by a factor of 11 (Ag^+ mass transport coefficient to Ag^+ under pure diffusion) and as a consequence the limiting current of Cu^{2+} is also increased by a factor of 2.8. Both Ag^+ and Au^{3+} can be used as a tracer for the potentiodynamic technique in the Cu/H_2SO_4 system.

3.2. *Polarization curves*

The voltammetry curves for the copper sulphate electrolyte, free of additives, with and without N_2 gas sparging are shown in Fig. 5. The curves overlapped at potentials below $-0.58\,V$ w.r.t. Hg/Hg_2SO_4, but beyond this potential depolarization occurs, indicating some mass transport contribution. The curves exhibited very good reproducibility. The value of $65\,mA\,cm^{-2}$ for the limiting current density calculated from Fig. 1 agrees with the value of $67\,mA\,cm^{-2}$ calculated.

A series of voltammetry experiments was also carried out at 40° C and 60° C and noticeable depolarization was evident (Fig. 6). At 60° C, sparging does not alter the position of the curve up to a current density of about $65\,mA\,cm^{-2}$.

3.3. *Electrodeposition tests*

Concentration polarization tends to promote growth of nodules that will eventually produce short circuits [4]. The mass transfer to the tips of these nodules is greatly enhanced relative to the rest of the cathode. This effect will be more severe when plating close to the limiting current where the concentration polarization is large and the deposit becomes rough or powdery and contaminated with components of the electrolyte and anode slimes.

A series of deposition tests was carried out on Ti blanks to investigate the effect of temperature, current density and gas sparging on deposit quality. Tem-

Table 4. Influence of N_2 gas sparging on the mass transfer parameters using the potentiodynamic measurement of a Ag^+ tracer on a platinum vertical electrode

Gas FR ($cc\,min^{-1}$)	$K_{Ag+} \times 10^4$ ($cm\,s^{-1}$)	$K_{Cu2+} \times 10^4$ ($cm\,s^{-1}$)	$I_{L,Cu2+}$ ($mA\,cm^{-2}$)	$[K/K^0]_{Ag}$	δ_{Ag+} (μm)	δ_{Cu2+} (μm)	I_L/I_L^0
22	29.0	17.6	190	11.0	35	27	2.8
48	36.9	22.4	242	14.0	28	22	3.6
98	43.5	26.4	285	16.5	23	18	4.3

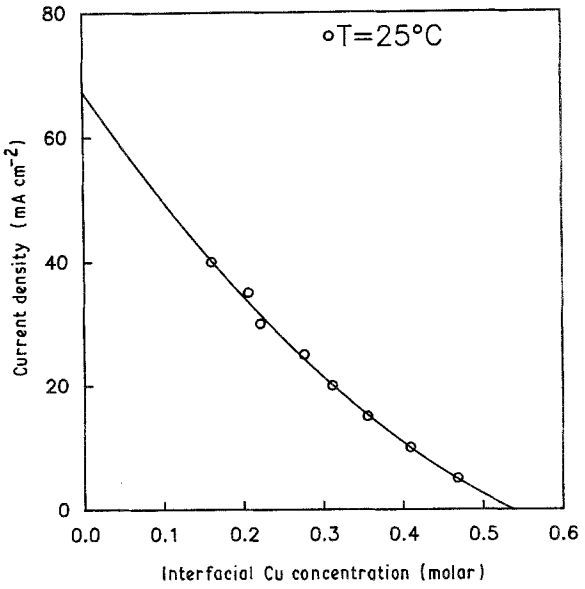

Fig. 1. Calculated interfacial Cu concentration change with the current density in an electrolyte containing 20 ppm Ag^+ as a tracer at different temperatures.

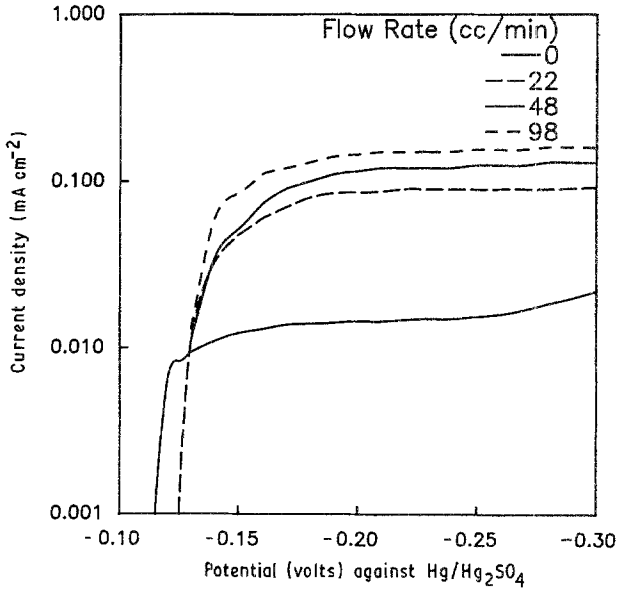

Fig. 3. Polarization curve for an electrolyte containing 40 ppm Ag^+ as a tracer at 25° C and different flow rates of N_2.

peratures of 25°, 40° and 60° C were used at current densities of 20, 35 and 50 mA cm^{-2}. Gas sparging was fixed at 48 cc min^{-1} (selected photomicrographs are presented in Figs 7 to 11). At low temperatures (i.e. 25° C) and relatively high current densities (i.e. 35 mA cm^{-2}) the deposit tends to exhibit rounded nodules. The quality of the electrodeposits was found to improve by increasing the electrolyte temperature from 25° to 60° C and by using gas sparging to eliminate the noduluation. These observations agree with the findings in which the Cu^{2+} mass transfer coefficient increases with temperature and agitation. For example at 25 mA cm^{-2} increasing the temperature from 25° to 45° C, the Cu^{2+} mass transfer coefficient increased from 4.5 × 10^{-4} to 5.8 × 10^{-4} cm s^{-1}.

In the polarization curve shown in Fig. 5, for the current density of 20 mA cm^{-2} with gas sparging there is no mass transfer contribution. Accordingly the deposits at this low current, with and without gas sparging, are quite similar but with somewhat less nodulation for the former (Fig. 7). At intermediate and high current densities (35 and 50 mA cm^{-2}), the mass transfer contribution is larger and the effect of gas sparging on the deposits is considerable. Increasing the current density at low temperature (25° C) leads to the formation of a rough and powdery deposit because of limited mass transfer of Cu^{2+} to the surface of the cathodes (Fig. 8). Roughness increases continuously (Fig. 9) with the increase in the ratio of the actual current density to the mass transfer controlled current density of Cu^{2+} ions ($I_{Cu^{2+}}/I_{L,Cu^{2+}}$). At a constant copper concentration, solution agitation by gas sparging is the dominant factor in determining the limiting current density of Cu^{2+} and, accordingly, it has a marked effect on the roughness of the deposit. Mass transfer determinations have shown that 2 to 5

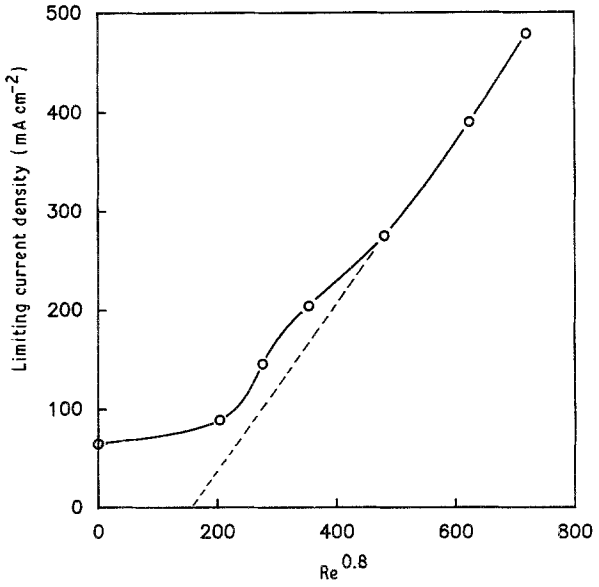

Fig. 2. Plot of diffusion limiting current density of Cu versus the Reynolds numbers for the forced circulation of electrolyte.

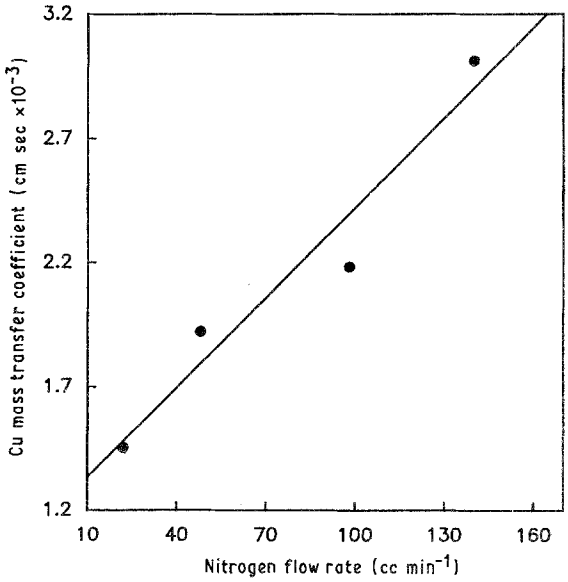

Fig. 4. Effect of N_2 flow rate on mass transfer coefficients of Cu estimated using Au^{3+} tracer.

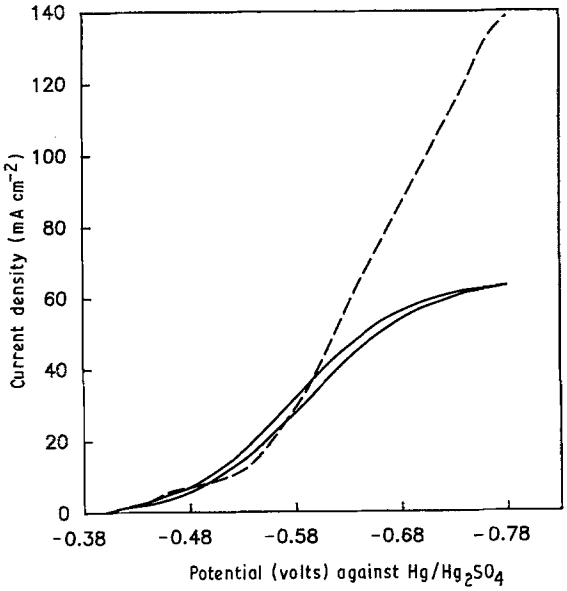

Fig. 5. Voltammograms obtained for electrolyte using gas sparging at T = 25° C and scan rate = 0.5 mV sec^{-1}.

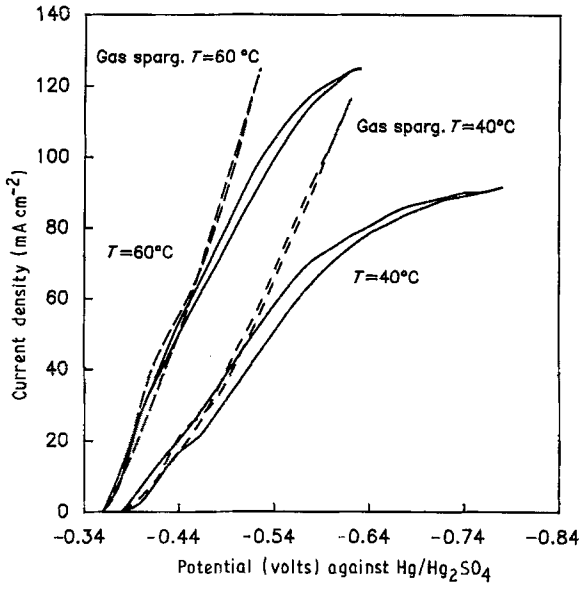

Fig. 6. Voltammograms obtained for electrolytes at various temperatures.

fold increases in the limiting current of Cu^{2+} occur using gas sparging rates of 22 to 140 cc min^{-1}.

A theoretical criterion for the transition from charge to mass transfer control has been presented by Robinson [12] who equated the rate constant for charge transfer expressed by the Tafel equation with the mass transfer coefficient derived from the Nernst approach. Then, assuming that the total overpotential is the sum of the concentration and activation overpotential a cubic equation was obtained which yielded the single real solution of $(I/I_L)_{crit} = 0.43$.

From this theoretical approach, it is obvious that at the critical current density of $0.43I_L$, mass transfer becomes appreciable. A limiting current of 65 mA cm^{-2}, was obtained experimentally at ambient temperature. The current density of 27 mA cm^{-2} ($0.42\,I_L$) is the point at which the polarization curves, obtained with and without sparging, begin to deviate from each other as shown in the experimental curve in Fig. 6. This point corresponds to a Cu^{2+} concentration at the interface of 16 g l^{-1}. Similarly, at 40° C the experimental limiting current density obtained was 90 mA cm^{-2} and the point at which the two polarization curves start to deviate was at 40 mA cm^{-2} ($0.44I_L$). Finally, at 60° C the limiting current density was of 130 mA cm^{-2} and the deviation point was at 55 mA cm^{-2} ($0.42I_L$).

According to Robinson the ratio $(I/I_L)_{crit}$ is independent of I_0. However, it has been shown [13] that $(I/I_L)_{crit}$ is difficult to predict and is higher for metals with low exchange current density, I_0, such as nickel or iron, than for copper and zinc. Nodular growth may be expected to occur when

$$(I/I_L)_{crit} = 1 - (I_0/I)^{x/\alpha}_{crit} \qquad (8)$$

where x is an empirical constant (0.3 to 0.4). Using the kinetic parameters reported for an electrolyte free of additives [14] I_0 = 11 mA cm^{-2} and I_L = 88 mA cm^{-2}, Equation 8 yields I = 14 mA cm^{-2} and $(I/I_L)_{crit}$ = 0.2 which is lower than the experimental value of $(I/I_L)_{crit}$ = 0.4. The low values of the ratio 0.2 to 0.4 obtained by the calculations are indicative of the importance of mass transfer. The absence of a specific identifiable value, such as I_L, makes it less useful in direct applications. The range of values causes other operating and chemical parameters, such as localized convective, additive and impurity effects or current distribution, to be more significant in the actual roughening process.

Gas sparging produced good deposits under con-

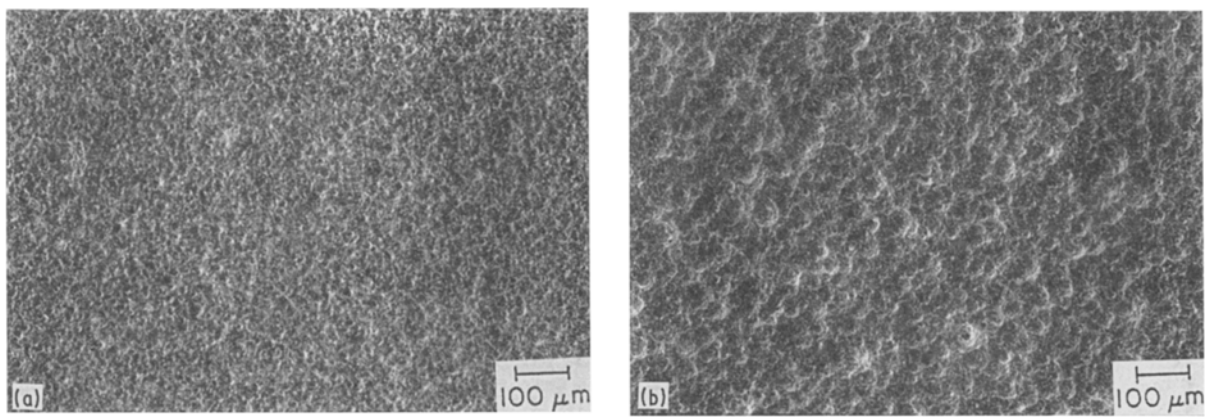

Fig. 7. Copper deposits obtained at T = 25° C and C.D. = 20 mA cm^{-2} (a) with gas sparging, (b) without gas sparging.

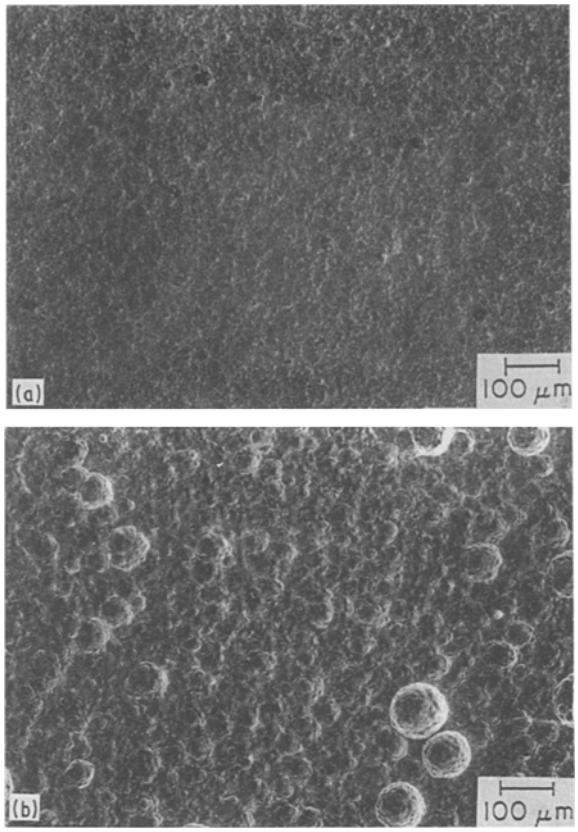

Fig. 8. Copper deposits obtained at $T = 25°C$ and C.D. = $35\,mA\,cm^{-2}$ (a) with gas sparging, (b) without gas sparging.

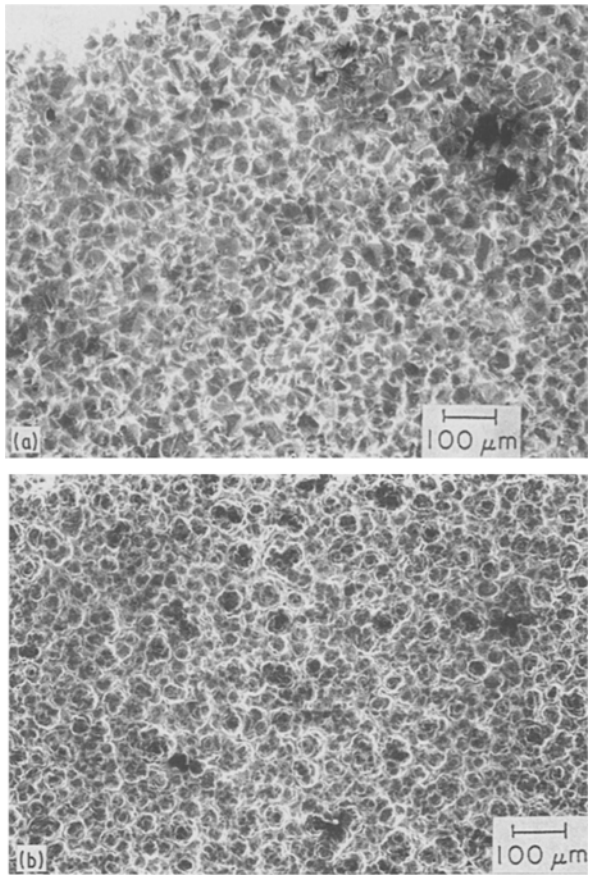

Fig. 10. Copper deposits obtained at $T = 40°C$ and C.D. = $50\,mA\,cm^{-2}$ (a) with gas sparging, (b) without gas sparging.

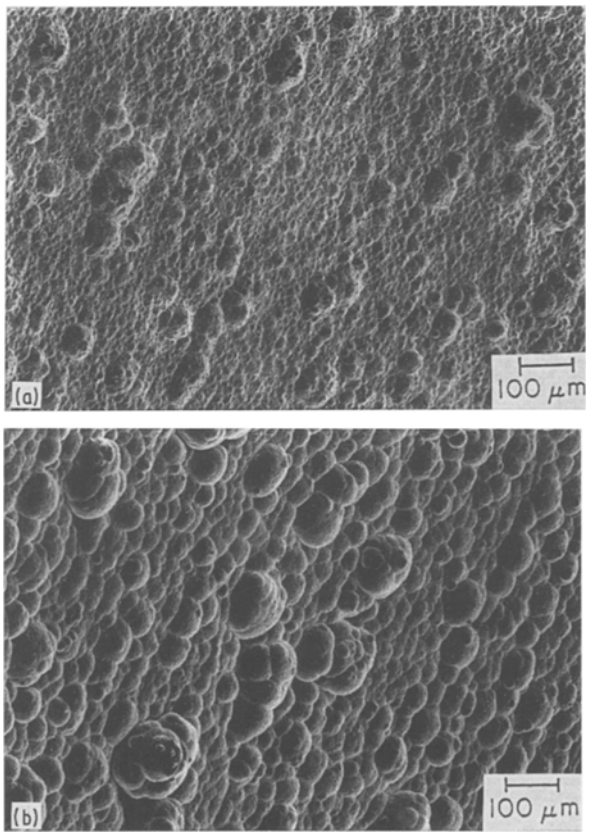

Fig. 9. Copper deposits obtained with gas sparging at $T = 25°C$. (a) C.D. = $73\,mA\,cm^{-2}$, (b) C.D. = $126\,mA\,cm^{-2}$.

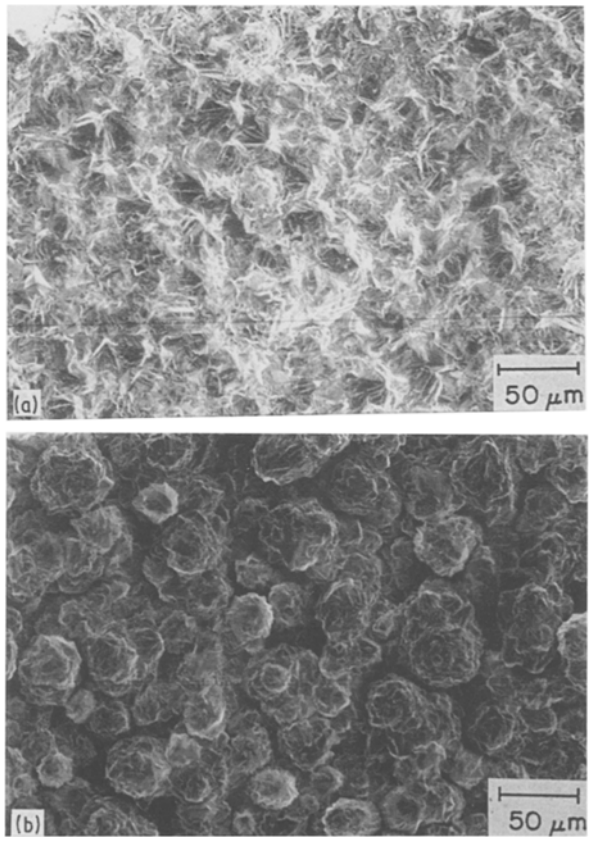

Fig. 11. Copper deposits obtained at $T = 60°C$ and C.D. = $80\,mA\,cm^{-2}$ (a) with gas sparging, (b) without gas sparging.

ditions in which conventional electrolysis would yield poor cathodes, for example, at 50 mA cm^{-2} and 25° C.

Again, at 40° C and for 35 mA cm^{-2} and 50 mA cm^{-2} where the mass transfer contribution is small, deposits with and without gas sparging looked similar (Fig. 10).

At 60° C, gas sparging does not produce a significant depolarization effect and deposits produced at 20, 35 and 50 mA cm^{-2} with and without sparging are therefore similar. However, deposits made at 80 mA cm^{-2} where a mass transfer contribution is evident, according to Fig. 2, show the effect of gas sparging (Fig. 11). Without gas sparging the deposit consists of separated individual grains, while the deposit produced under the same condition but with gas sparging is highly crystallized.

Cathodic current efficiency (CE) was determined for each test. The CE tended to decrease with sparging. The deposition of Cu^{2+} has been proposed to occur in a two step mechanism according to the following equations [15, 16]

$$Cu^{2+} + e = Cu \quad (a)$$

$$Cu^{+} + e = Cu \quad (b)$$

For copper plating, reaction (a) consistutes the kinetically limiting process [17]. Thus, reaction (b) is in equilibrium with the copper surface and the Cu^{+} concentration near the electrode surface is small. The existence of Cu^{+} has been experimentally confirmed by using a rotating ring disc technique. Furthermore, the CE for copper deposition in a pure electrolyte free of additives is close to 100%. For gas sparging, the concentration of Cu^{+} increases and may be lost to the bulk solution by convection or diffusion resulting in a loss of current efficiency.

4. Conclusions

The concentration of copper at the electrode/electrolyte interface was estimated for each applied current density. The limiting current density of the system was determined by extrapolation of the current density to zero copper concentration at the interface. The estimated limiting current density was 67 mA cm^{-2} for an electrolyte containing 36 g l^{-1} Cu^{2+} at 25° C and agrees with the value of 65 mA cm^{-2} directly obtained from a steady-state polarization curve for copper deposition up to the limiting current.

Calculations of the Sherwood number for laminar natural convection, according to Wilke's approach, agree with the experimentally determined Sherwood number. Results indicate that when the current density was increased from 5 to 40 mA cm^{-2}, approaching the limiting current density, the agreement between the predicted and calculated Sherwood number, improves. It has been shown that natural convection provides an effective way of stirring the electrolyte, decreasing the diffusion layer thickness by a factor of one half (from 176 to 94 μm) when the current density was varied from 5 to 40 mA cm^{-2}. For further decreases of the diffusion layer thickness (by a factor of 10) forced convection such as gas sparging is required.

The limiting current of Ag^{+} was determined potentiodynamically in both quiescent and agitated electrolytes by forced circulation and gas sparging. The limiting current of Cu^{2+} was estimated under those conditions and compared with the limiting current obtained under conditions of natural convection. The limiting current density of Cu^{2+} was significiantly enhanced by both systems of agitation, as expected. Gas sparging in the range of 22 to 98 cc min^{-1} gave values of copper mass transfer coefficients of 17.6×10^{-4} to 26.4×10^{-4} cm s^{-1}, which are in the range of values reported [5] of 10×10^{-4} to 40×10^{-4} cm s^{-1}. The similar values obtained indicate that laboratory sized experiments probably are valid for making first approximations of mass transport effects on deposition. Deposits at high temperature with and without gas sparging looked quite similar. It seems that gas sparging only helps when there is some mass transfer contribution. At 60° C, sparging does not depolarize in the same amount as at room temperature.

The current efficiency with gas sparging is lower than the current efficiency in a conventional electrolytic process. This could be explained by the stabilization of Cu^{+} near the cathodic surface.

The transition from charge to mass transfer takes place at about 40% of the limiting current which is a theoretical value that agrees with the experimental polarization curves since below this value there is no mass transfer contribution. This transition value holds even at increased rates of gas sparging and also agrees with the practical limit for copper plating which is about 50% of the limiting current density. Deposits made below this value with and without gas sparging looked similar. Above this transition value there was an increase of the nodule population and as the ratio I/I_L approached unity, a powdery loose deposit resulted.

References

[1] W. Harvey and L. Hsueh, *CIM Bull.* **69** (1976) 109.
[2] W. Cooper, *J. Appl. Electrochem.* **15** (1985) 789.
[3] W. Cooper and K. Mishra, *Hydrometallurgy* **17** (1987) 305.
[4] W. W. Harvey, M. R. Randlett and K. I. Bangerskis, *J. Metals* **30** (1978) 32.
[5] V. A. Ettel, A. S. Gendron and B. V. Tilak, 102nd AIME (1973).
[6] *Idem, J. Electrochem. Soc.* **121** (1974) 867.
[7] T. J. O'Keefe, S. F. Chen, J. S. Cuzmar and V. A. Ettel, 'Hydrometallurgical Reactor Design' (edited by R. G. Bautista, R. J. Wesely and G. W. Warren) TMS, Warrendale, PA, (1987) p. 359.
[8] C. R. Wilke, M. Eisenberg and C. W. Tobias, *J. Electrochem. Soc.* **49** (1953) 513.
[9] E. J. Fenech and C. W. Tobias, *Electrochim. Acta* **2** (1960) 311.
[10] D. J. Pickett and K. L. Ong, *ibid.* **19** (1974) 875.
[11] H. Y. Sohn and M. E. Wadsworth, 'Rate Processes of Extractive Metallurgy', Plenum, New York (1976) p. 141.
[12] D. J. Robinson, PhD Dissertation, Univ. Sheffield (1970).
[13] J. M. West, 'Electrodeposition and Corrosion Process', 2nd Edn, Van Nostrand Reinhold, New York (19709) p. 125.
[14] P. Padilla, F. A. Olson and T. N. Andersen, 'Energy Reduction Techniques in Metal Electrochemical Processes', (edited by R. G. Bautista and R. J. Wesely) TMS-AIME, New York (1985) p. 179.
[15] E. Mattson and J. O'M. Bockris, *Trans. Farday Soc.* **54** (1958) 1586.
[16] I. R. Burrows, J. A. Harrison and J. Thompson, *Electroanal. Chem. Interfacial Electrochem.* **58** (1975) 241.
[17] J. R. White, *J. Appl. Electrochem.* **15** (1987) 977.